Study on Characteristics of Various RF Transmission Line Structures on PES Substrate for Application to Flexible MMIC

Young Yun, Hong Seung Kim, and Nakwon Jang

In this work, the coplanar waveguide is fabricated on a PES (poly[ether sulfone]) substrate for application to a flexible monolithic microwave integrated circuit, and its RF characteristics were thoroughly investigated. The quality factor of the coplanar waveguide on PES is 40.3 at a resonance frequency of 46.7 GHz. A fishbone-type transmission line (FTTL) structure is also fabricated on the PES substrate, and its RF characteristics are investigated. The wavelength of the FTTL on PES is 5.11 mm at 20 GHz, which is 55% of the conventional coplanar waveguide on PES. Using the FTTL, an impedance transformer is fabricated on PES. The size of the impedance transformer is 0.318 mm × 0.318 mm, which is 69.2% of the size of the transformer fabricated by the conventional coplanar waveguide on PES. The impedance transformer showed return loss values better than –12.9 dB from 5 GHz to 50 GHz and an insertion loss better than –1.13 dB in the same frequency range.

Keywords: RF, transmission line, poly(ether sulfone), PES, monolithic microwave integrated circuit, MMIC, coplanar waveguide, fishbone-type transmission line, FTTL.

Manuscript received Feb. 03, 2013; revised Mar. 21, 2013; accepted Apr. 02, 2013.

This research was financially supported by the Ministry of Education, Science Technology (MEST) and National Research Foundation of Korea (NRF) through the Human Resource Training Project for Regional Innovation. This research was also supported by Basic Science Research Program through the National Research Foundation of Korea (NRF) funded by the Ministry of Education, Science and Technology (2010-0007452).

Young Yun (phone: +82 51 410 4426, yunyoung@hhu.ac.kr), Hong Seung Kim (hongseung@hhu.ac.kr), and Nakwon Jang (nwjang@hhu.ac.kr) are with Korea Maritime University, Busan, Rep. of Korea.

I. Introduction

This paper is an extension of an article previously published in conference proceedings [1]. Flexible electronics has drawn significant attention owing to its variety of applications, such as flexible displays, smart tags, and wearable products [2]-[9]. Particularly for the development of transparent flexible displays with mobile communication functions, RF devices should be integrated into transparent flexible substrates. For the realization of flexible monolithic microwave integrated circuits (MMICs), all passive devices are fabricated on the transparent flexible substrates, and such active devices as transistors are transferred to flexible substrates using a wafer transfer technique [10]. In other words, active devices are fabricated on rigid substrates, such as silicon, and then the active devices are transferred from the rigid substrates to flexible substrates through a flip chip bonding process. Before the active devices are transferred to the flexible substrates, the rigid substrates on which active devices were fabricated are made very thin by using an etching process because the active devices should have the same flexibility as the flexible substrates.

Recently, PES (poly[ether sulfone]) has drawn attention for its application to transparent flexible displays due to its notable heat-resisting property, high transparency, and flexibility [5]-[8]. Concretely, the glass transition temperature (T_g) of PES is 230°C, and it shows stable electrical and mechanical properties at high temperatures, which enables the fabrication of electron devices at a relatively high temperature [5]-[8]. For a heat-resisting property with a short duration, electrical and mechanical properties of PES do not change, even at 300°C.

Therefore, unlike other flexible substrates, such as PC (polycarbonate) and PET (poly[ethylene terephthalate]), the soldering and bonding process for the electron devices on PES can be easily performed, which facilitates a packaging process of electron devices on a semiconducting substrate. In addition, a very thin PES substrate with a thickness of less than 100 μm can be used for the fabrication of electron devices due to its tenacity, which is very effective for the miniaturization of RF components. Furthermore, PES shows a contraction ratio of less than 0.2%, even if it is exposed to a high temperature environment for a long time, which enables such a precise process as the microelectromechanical system process. Additionally, various techniques to improve the coefficient of thermal expansion of PES have recently been studied.

Herein, we use the PES substrate for application in flexible mobile communication devices [9]. Coplanar waveguides are fabricated on the PES substrate, and their RF characteristics are extracted using theoretical and experimental analysis. In addition, a fishbone-type transmission line (FTTL) is properly designed for wavelength reduction, and its RF characteristics are also thoroughly investigated. In addition, a miniaturized impedance transformer employing the FTTL on PES is developed for application to flexible RF matching components.

II. RF Characteristics of Coplanar Waveguide on PES Substrate

Figure 1 shows a photograph of the coplanar waveguide fabricated on PES. Au/Ti is deposited on the PES substrate with a thickness of 200 μm, and the thickness of the Au/Ti is 2 μm. The line width (*W*) is 30 μm, 50 μm, and 70 μm. The distance between the line and ground plane is 80 μm, and the width of the ground plane is 120 μm.

We measure the insertion loss of the coplanar waveguide with various line widths. Figure 2 shows the measured insertion loss per 1 mm of the coplanar waveguide on PES. As shown in this figure, the coplanar waveguide on PES shows very low loss. Concretely, it shows an insertion loss lower than 0.7 dB/mm up to 50 GHz. A commercial silicon substrate shows an insertion loss of 3 dB/mm at 50 GHz [11], [12]. The coplanar waveguide on a GaAs substrate shows an insertion loss of less than 0.42 dB in a frequency range of 5 GHz to 25 GHz [13]. As shown in Fig. 2, the coplanar waveguide on the PES substrate shows an insertion loss of less than 0.45 dB in the same frequency range. These results indicate that the PES shows an insertion loss that is much lower than that of the silicon substrate and that is comparable to the commercial GaAs compound semiconducting substrate. We extract attenuation constant α from the insertion loss data using the transmission line theory. The electromagnetic wave on the

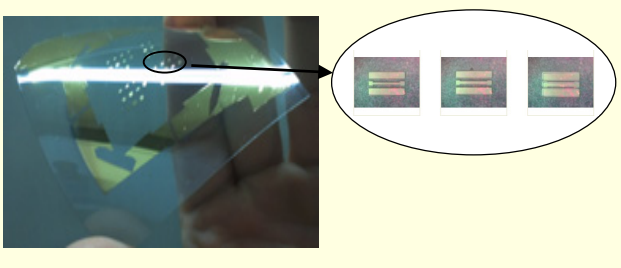

Fig. 1. Photograph of coplanar waveguides fabricated on PES.

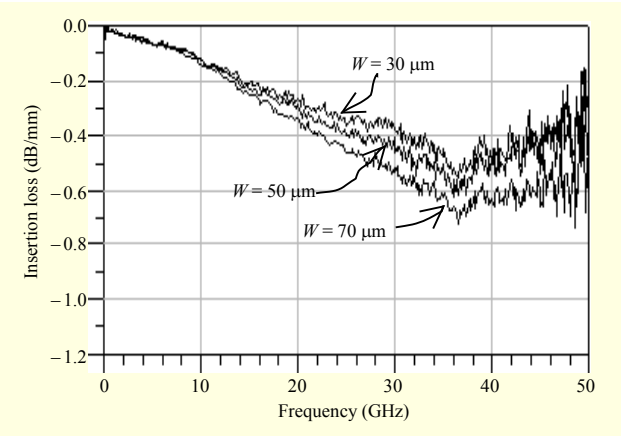

Fig. 2. Measured insertion loss per 1 mm of coplanar waveguide on PES substrate.

transmission line can be expressed as follows:

$$E = E_0 e^{-(\alpha + j\beta)z}, \tag{1a}$$

$$H = H_0 e^{-(\alpha + j\beta)z}, \tag{1b}$$

where α and β are the attenuation constant and propagation constant, respectively. If the electromagnetic wave propagates on a line with length l, insertion loss S_{21} can be given by

$$S_{21}(\mathrm{dB}) = 10\log|e^{-\alpha l}|^2|e^{-j\beta l}|^2 = 10\log|e^{-\alpha l}|^2, \ (|e^{-j\beta l}|^2 = 1). \tag{2}$$

From (2), we can obtain the following attenuation constant:

$$\alpha = -0.5\ln[10^{0.1\times S_{21}(\mathrm{dB})}]/l \quad (\mathrm{Np/mm}). \tag{3}$$

Figure 3 shows measured propagation constant α of the coplanar waveguide on PES. As shown in this figure, the coplanar waveguide on PES shows α lower than 0.085 Np/mm up to 50 GHz, which is much lower than that of the silicon substrate. The commercial silicon substrate shows an α of 0.32 Np/mm at 50 GHz [11], [12]. This low loss of the coplanar waveguide on PES originates from the excellent electrical insulating properties. In the case that the coplanar waveguide is on the silicon substrate, there is a current flowing from the line to the ground plane through the silicon substrate

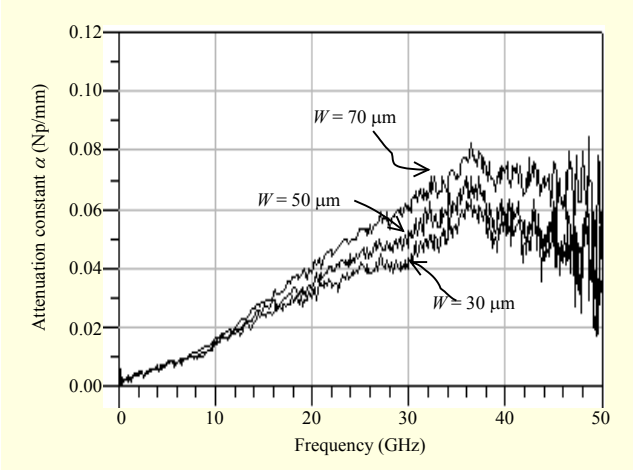

Fig. 3. Measured attenuation constant α of coplanar waveguide on PES substrate.

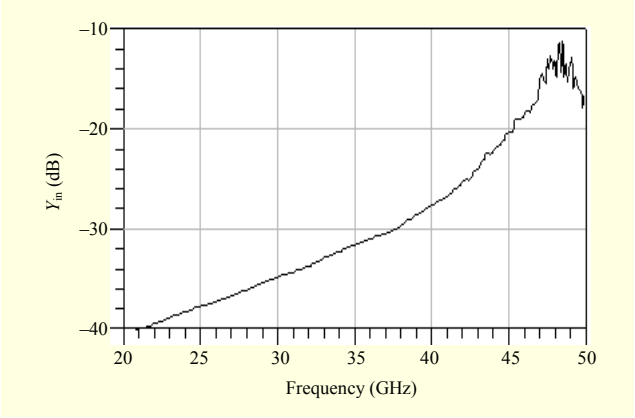

Fig. 4. Measured input admittance (Y_{in}) of one-port open-ended coplanar waveguide on PES.

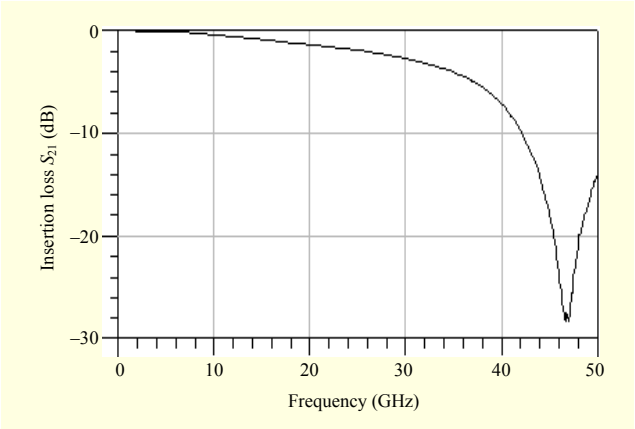

Fig. 5. Measured two-port insertion loss S_{21} of two-port open-ended coplanar waveguide on PES.

due to a relatively high conductivity of the silicon substrate, which causes a relatively high loss of electromagnetic energy [11], [12]. In the case that the coplanar waveguide is on PES, however, there is no current flowing from the line to ground plane through the PES substrate due to its excellent electrical insulating characteristic. We must pay attention to one point from the above-mentioned results. The attenuation is lowest for the widest line below 2.5 GHz. However, as the frequency increases and more energy is coupled in the substrate, the attenuation rises such that the narrowest line has the lowest attenuation above approximately 14 GHz. This tendency of the loss characteristic was also observed from other semiconducting materials [12].

We also investigate the quality factor (Q-factor) of the coplanar waveguide on PES. The Q-factor of the transmission line is derived from the resonance characteristic of a stub with a length of a quarter wavelength. The Q-factor is extracted by the ratio of –3-dB bandwidth to resonance frequency f_0; in other words, $Q = f_0/\Delta f\_{3dB}$. This Q-factor can be obtained from a one-port or two-port quarter wavelength open stub. Figure 4 shows the input admittance of the one-port open-ended coplanar waveguide on PES, its width 70 μm and length 1,000 μm. The one-port open-ended coplanar waveguide on PES shows a Q-factor of 38.3 at a resonance frequency of 49.8 GHz. Using a two-port open-ended coplanar waveguide on PES, we also extract the Q-factor of the coplanar waveguide on PES to reconfirm the loss characteristic of the PES substrate. Figure 5 shows two-port insertion loss S_{21} of the two-port open-ended coplanar waveguide on PES. The Q-factor is 40.3 at a resonance frequency of 46.7 GHz. Table 1 shows Q-factors of transmission lines on PES and a silicon substrate. As shown in this table, the transmission line on PES shows a Q-factor much higher than that on the silicon substrate. These results indicate

Table 1. Q-factors of transmission line on PES and silicon substrate.

Substrate	Q-factor	Frequency	Type	Method
PES (this work)	38.3	49.8 GHz	Coplanar waveguide	One-port open-ended ($f_0/\Delta f\_{3dB}$)
PES (this work)	40.3	46.7 GHz	Coplanar waveguide	Two-port open-ended ($f_0/\Delta f\_{3dB}$)
Silicon [12]	6.3	40 GHz	Microstrip line	One-port open-ended ($f_0/\Delta f\_{3dB}$)
Silicon [14]	13	47 GHz	Microstrip line	Equivalent circuit (ω_L; ω_R)
Silicon [14]	23	47 GHz	Coplanar waveguide	Equivalent circuit (ω_L; ω_R)

that the RF passive components on the PES substrate can be applied to the millimeter wave as well as the microwave due to its very low loss.

Figure 6 shows the wavelength of the coplanar waveguide on PES. As shown in this figure, the coplanar waveguide on PES shows a wavelength of 4 mm to 6.2 mm from 30 GHz to

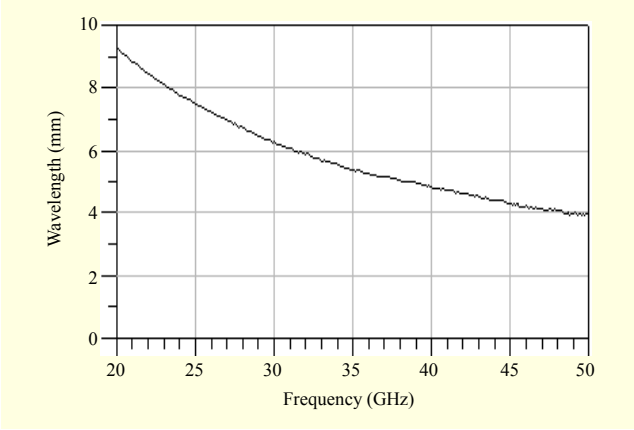

Fig. 6. Measured wavelength of coplanar waveguide on PES.

50 GHz. For a high integration of an RF circuit on PES, bulky passive components as well as transistors should be integrated in the PES substrate. One of the largest RF components is the branch-line coupler, which is usually fabricated on a printed circuit board, not on a semiconducting substrate, due to its large size. To evaluate the integration capacity of RF passive components on the PES substrate, we calculate the size of branch-line couplers consisting of $\lambda/8$ transmission lines [15] from the wavelength. The size of conventional branch-line couplers consisting of $\lambda/8$ transmission lines on PES is listed in Table 2. As shown in this table, the size of branch-line couplers is smaller than 0.619 mm × 0.619 mm in a frequency range of 30 GHz to 50 GHz, which indicates that bulky passive components can be integrated in the PES substrate with a small chip size in the millimeter wave frequency range.

Figure 7 shows high frequency effective permittivity ε_{eff} of the coplanar waveguide on PES. The effective permittivity is obtained from the following equation.

$$\varepsilon_{\text{eff}} = \left(\frac{2\pi}{\omega\lambda} \times \frac{1}{\sqrt{\varepsilon_0 \mu_0}} \right)^2, \tag{4}$$

where ω, λ, ε_0, and μ_0 is angular frequency, wavelength, permittivity, and permeability of air, respectively. As shown in this figure, the coplanar waveguide on PES shows the ε_{eff} of 2.35 to 2.97 from 10 GHz to 50 GHz. The coplanar waveguide on the silicon substrate shows a strong frequency dispersion characteristic [12]. This tendency originates from the existence of various propagation modes on the oxide/silicon substrate. Concretely, skin-effect mode and slow-wave mode of the propagation exist in addition to the quasi-transverse electromagnetic (quasi-TEM) mode on the oxide/silicon substrate, which causes a large change in ε_{eff} between 1 GHz and 20 GHz [12]. On the other hand, as shown in Fig. 7, the coplanar waveguide on PES shows a very weak frequency dispersion characteristic compared with the silicon substrate

Table 2. Size of conventional branch-line couplers consisting of $\lambda/8$ transmission lines on PES.

Frequency	Branch-line coupler size
30 GHz	0.619 mm × 0.619 mm
40 GHz	0.36 mm × 0.36 mm
50 GHz	0.239 mm × 0.239 mm

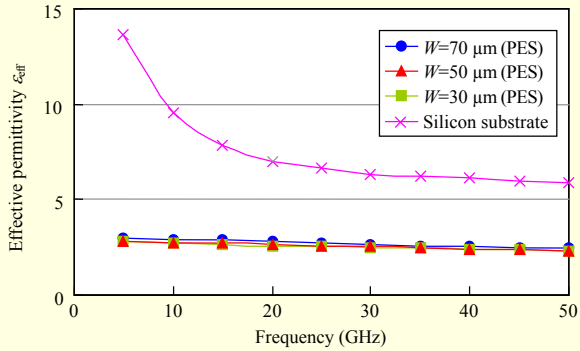

Fig. 7. Measured ε_{eff} of coplanar waveguide on PES and silicon substrate.

because the quasi-TEM mode dominantly propagates on the metal/high-insulating substrate structure [16]. These results indicate that the coplanar waveguide on PES is suitable for broadband applications due to its very weak frequency dispersion characteristic.

As is well known, the basic RF parameters of a microwave transmission line are expressed by a periodic capacitance (C) and periodic inductance (L) of an LC equivalent circuit [17]. Therefore, we extract the equivalent C and L from the coplanar waveguide on PES. For a low loss transmission line, propagation constant β and characteristic impedance Z_0 are given by [17]

$$\beta \approx \omega\sqrt{LC}, \tag{5}$$

$$Z_0 = \sqrt{\frac{L}{C}}. \tag{6}$$

Using the above equations, we can obtain the following result.

$$C = \frac{L}{Z_0^2} = \frac{\beta}{\omega Z_0} = \frac{1}{\omega Z_0} \times \frac{2\pi}{\lambda}, \tag{7}$$

$$L = CZ_0^2 = \frac{Z_0}{\omega} \times \frac{2\pi}{\lambda}. \tag{8}$$

Figures 8(a) and 8(b) show the equivalent C and L of the coplanar waveguide on PES. The coplanar waveguide with a line width of 70 μm shows the capacitance value of

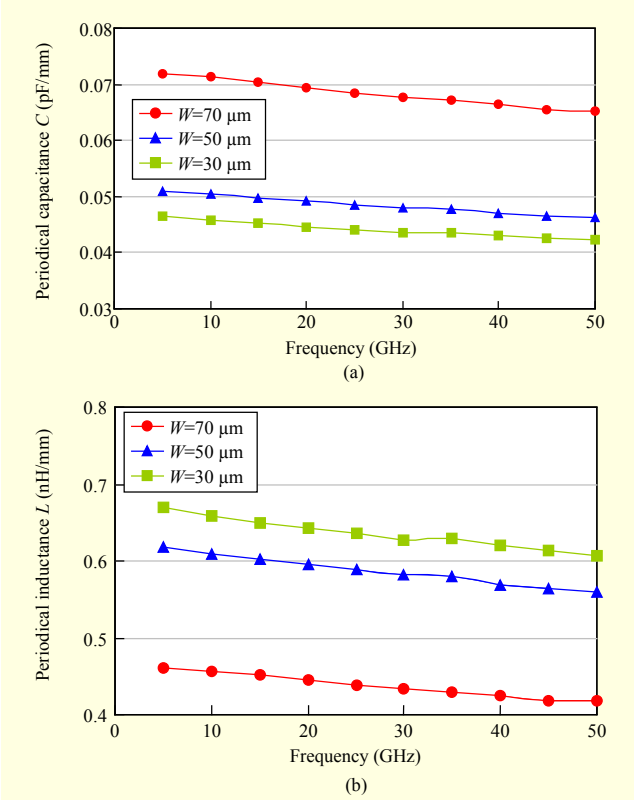

Fig. 8. Measured equivalent circuit parameters of coplanar waveguide on PES: (a) equivalent C per unit length and (b) equivalent L per unit length.

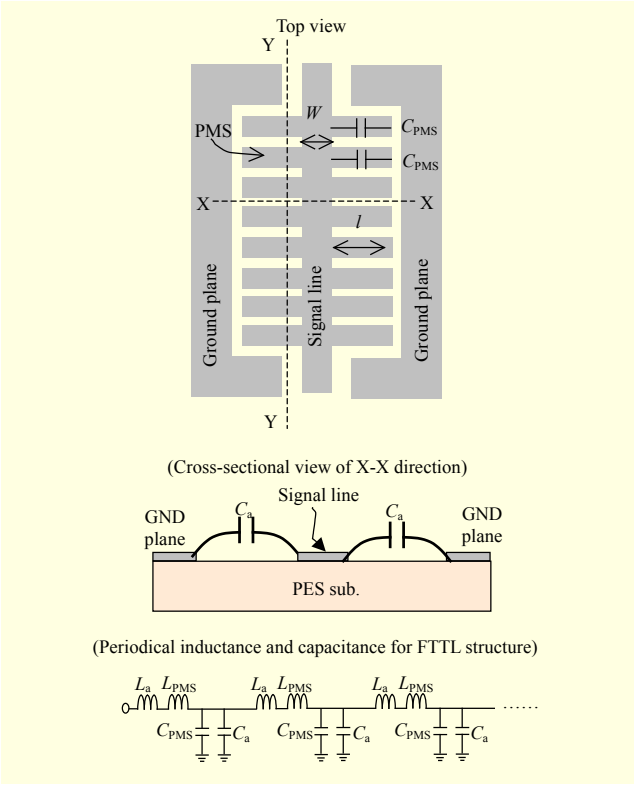

Fig. 9. Structure of FTTL on PES.

0.065 pF/mm to 0.072 pF/mm and the inductance value of 0.42 nH/mm to 0.46 nH/mm from 5 GHz to 50 GHz. The coplanar waveguide with a line width of 30 μm shows the capacitance value of 0.042 pF/mm to 0.047 pF/mm and the inductance value of 0.61 nH/mm to 0.67 nH/mm from 5 GHz to 50 GHz. As shown in this figure, as the line width becomes wider, the capacitance increases and the inductance decreases. This tendency has been observed in other semiconducting materials [18].

III. RF Characteristics of Coplanar Waveguide Employing Fishbone-Type Transmission Line on PES

According to the measured result, the wavelength of the coplanar waveguide on the silicon substrate and on the PES substrate is 5.71 mm and 9.29 mm at 20 GHz, respectively. For a miniaturization of RF components, the wavelength should be shortened. Therefore, in this work, a transmission line employing a periodic structure on PES is proposed to shorten the wavelength because a properly designed periodic structure causes a slow-wave effect and reduces the wavelength [11]. The guided wavelength, λ_g, for the transmission line can be expressed as follows [17]:

$$\lambda_g = \frac{1}{f\sqrt{LC}}, \tag{9}$$

where L and C correspond to the periodic inductance and periodic capacitance of the LC equivalent circuit of the transmission line, and f is an operating frequency. From (9), we can see that periodic C and L should be increased to decrease λ_g. In this work, we propose a fishbone-type transmission line (FTTL) on PES. Figure 9 shows the structure of the FTTL on PES. As shown in this figure, the FTTL consists of a fishbone-type center line and ground planes. The fishbone-type center line consists of signal line and periodic metal strips (PMSs). The conventional coplanar waveguide has only a periodic capacitance C_a between the line and ground plane, whereas the FTTL has periodic shunt capacitance C_{PMS} in addition to C_a because each PMS operates as a periodic open stub capacitor in the operating frequency. In addition, the conventional coplanar waveguide has only a periodic inductance L_a due to the current flowing across the signal line, whereas the FTTL has inductance L_{PMS} in addition to L_a due to the current flowing across the PMS. Therefore, the FTTL has higher C and L than the conventional coplanar waveguide has, which leads to an enhancement of effective permittivity and a reduction of wavelength. To confirm this assertion, we extract the

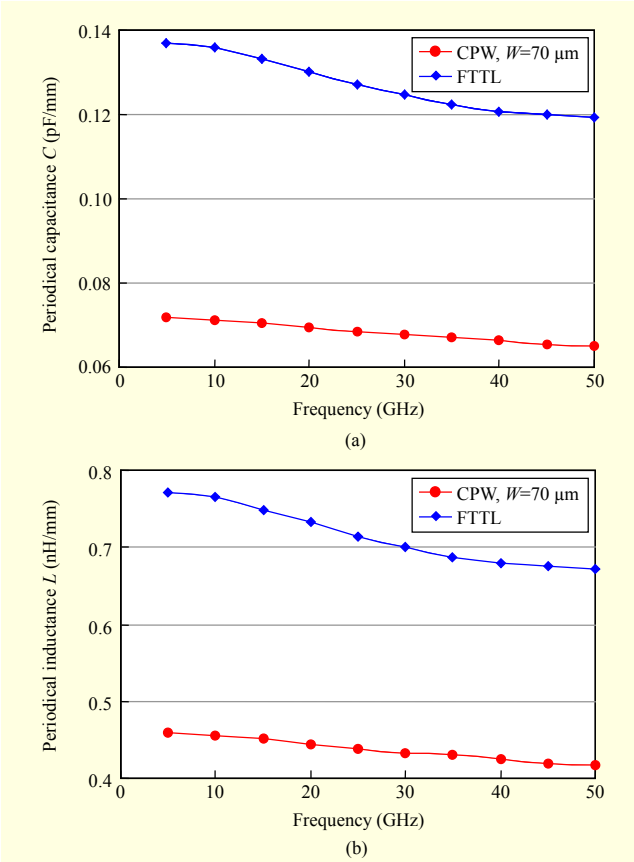

Fig. 10. Measured equivalent circuit parameters of FTTL and conventional coplanar waveguide on PES: (a) equivalent C per unit length and (b) equivalent L per unit length.

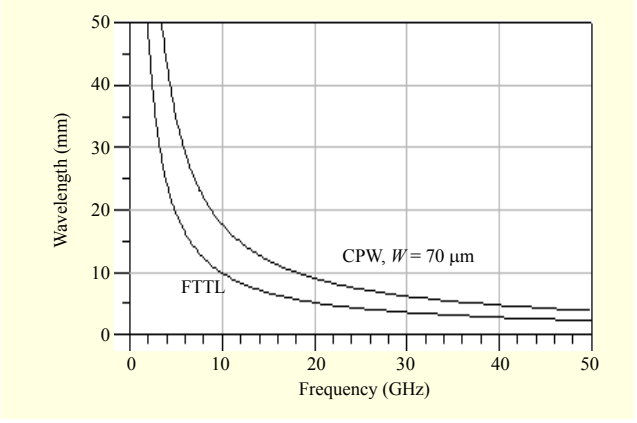

Fig. 11. Measured wavelength of the FTTL and conventional coplanar waveguide on PES.

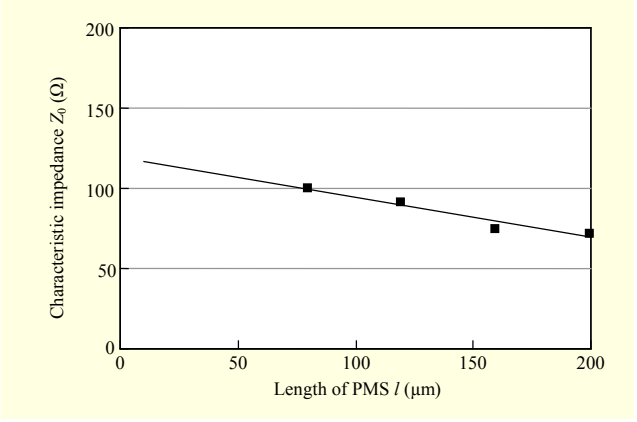

Fig. 12. Measured Z_0 of FTLCGP structure on PES.

equivalent capacitance of the FTTL and the conventional coplanar waveguide on PES using (7) and (8). Figures 10(a) and 10(b) show the equivalent C and L of the FTTL structure and the conventional coplanar waveguide on PES. For a fabrication of the FTTL on PES, Au/Ti is deposited on the PES substrate with of a thickness of 200 μm, and the thickness of the Au/Ti is 2 μm. For the FTTL, the length and width of the PMS is 160 μm and 30 μm, respectively, and the signal line width, W, and length is 70 μm and 500 μm, respectively. For a fair comparison, the data of the coplanar waveguide with the same line width (70 μm) is used. As shown in this figure, the FTTL shows capacitance and inductance values much higher than those of the conventional coplanar waveguide. Concretely, the FTTL on PES shows the respective capacitance and inductance to be 0.12 pF/mm to 0.137 pF/mm and 0.67 nH/mm to 0.77 nH/mm from 5 GHz to 50 GHz, and the conventional coplanar waveguide on PES shows the respective capacitance and inductance to be 0.065 pF/mm to 0.072 pF/mm and 0.42 nH/mm to 0.46 nH/mm at the same frequency range.

Figure 11 shows a comparison of wavelengths for the FTTL and the conventional coplanar waveguide on PES. As shown in this figure, the FTTL structure shows a wavelength much shorter than that which the conventional coplanar waveguide shows. Concretely, the wavelength of the conventional coplanar waveguide on PES is 9.29 mm at 20 GHz, whereas the wavelength of the FTTL on PES is 5.11 mm at the same frequency, which is 55% of conventional coplanar waveguide on PES.

From Fig. 9, we can see that an increase of the length of PMS, l, results in an enhancement of periodic shunt capacitance C_{PMS} due to an increase in the open stub length. Therefore, the characteristic impedance, Z_0, of the FTTL can be easily controlled by changing l because Z_0 depends on a C of the transmission line, as shown in (6). A dependence of Z_0 on l is shown in Fig. 12, where signal line width W is fixed to 70 μm. These results indicate that miniaturized flexible RF components with various impedance values can be realized on the PES substrate by using the FTTL.

Figure 13 shows propagation constant β of the FTTL structure and the conventional coplanar waveguide on PES. As

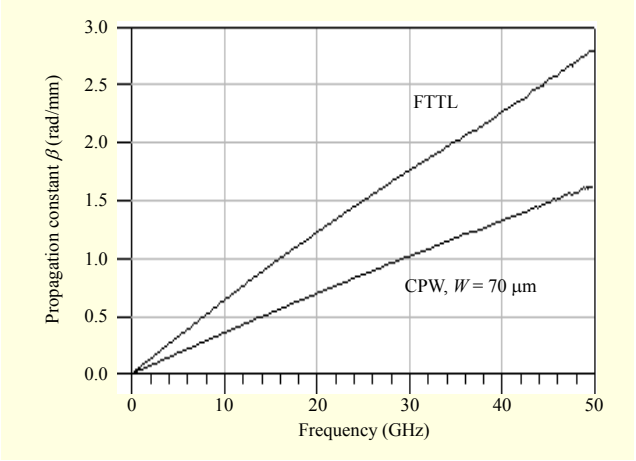

Fig. 13. Measured β of FTTL and conventional coplanar waveguide on PES.

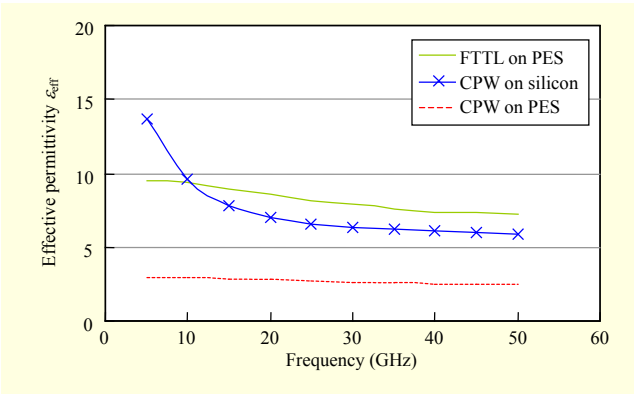

Fig. 14. Measured ε_{eff} of FTTL and conventional coplanar waveguide on PES.

shown in Fig. 13, the FTTL shows much higher propagation constant β than the conventional coplanar waveguide shows. Concretely, the FTTL on PES shows a β of 0.64 rad/mm to 2.81 rad/mm from 10 GHz to 50 GHz, whereas the coplanar waveguide on PES shows a β of 0.35 rad/mm to 1.64 rad/mm from 10 GHz to 50 GHz. These results indicate that slow-wave mode exists on the FTTL due to its periodic structure, which is favorable for a miniaturization of RF components.

Figure 14 shows effective permittivity ε_{eff} of the FTTL and the conventional coplanar waveguide on PES. For a comparison, the ε_{eff} of the conventional coplanar waveguide on the silicon substrate is also plotted. As shown in this figure, the FTTL shows a much higher effective permittivity than does the conventional coplanar waveguide on PES due to an enhancement of the C and L. Concretely, the FTTL shows an ε_{eff} of 7.2 to 9.5 from 5 GHz to 50 GHz, whereas the coplanar waveguide on PES shows an ε_{eff} of 2.45 to 2.97 within the same frequency range. In addition, it shows a higher ε_{eff} higher than the coplanar waveguide shows on the silicon substrate at a frequency range higher than 10 GHz. An increase in the effective permittivity of the FTTL results in a reduction of the wavelength.

Table 3. Insertion loss of various transmission lines with length of $\lambda/4$.

Frequency	FTTL on PES	Conventional CPW on PES	Conventional CPW on silicon
10 GHz	0.86 dB	1.34 dB	2.81 dB
20 GHz	1.31 dB	1.55 dB	2.54 dB
30 GHz	1.44 dB	1.69 dB	2.16 dB
40 GHz	1.18 dB	1.53 dB	1.89 dB
50 GHz	0.91 dB	1.61 dB	1.70 dB

In this work, we also investigate the loss of the FTTL. For a fair loss comparison, the loss of the FTTL and that of the conventional coplanar waveguide with the same electrical length should be compared because the FTTL shows a much shorter wavelength than the conventional coplanar waveguide shows. Therefore, the loss of the FTTL and that of the conventional coplanar waveguide with a length of $\lambda/4$ are compared, and the results are shown in Table. 3. For a comparison, the data of the coplanar waveguide on the silicon substrate is also listed because the silicon substrate is the most popular for application to RF components. As shown in this table, the FTTL on PES shows very low loss compared with that which the silicon substrate shows, which is comparable to that which the conventional coplanar waveguide on PES shows.

IV. RF Characteristics of Impedance Transformer Employing FTTL on PES

Using the FTTL structure on PES, a miniaturized impedance transformer is developed for flexible MMIC applications. Figure 15 shows a photograph of a single section $\lambda/4$ impedance transformer on the PES substrate. Au/Ti is deposited on the PES substrate with of a thickness of 200 μm, and the thickness of the Au/Ti is 2 μm. Characteristic impedance Z_0 of the transformer is given by $Z_0 = (Z_{c1} \times Z_{c2})^{0.5}$ [17], where Z_{c1} and Z_{c2} are the source impedance and load impedance, respectively, as shown in Fig. 15. In this work, the impedance transformer is designed to transform an impedance of 75 Ω into a standard impedance of 50 Ω. Therefore, Z_{c1} is 75 Ω, Z_{c2} is 50 Ω, and Z_0 is 61 Ω. For a Z_0 of 61 Ω, the length of the PMS is 230 μm and W is 70 μm. For a center frequency of 30 GHz, the length of the $\lambda/4$ transformer is 0.6 mm. Therefore, the size of the impedance transformer is 0.318 mm ×

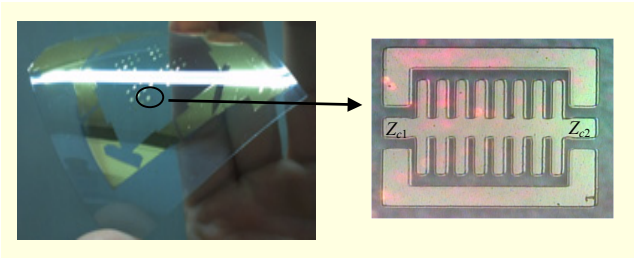

Fig. 15. Photograph of single section $\lambda/4$ impedance transformer employing FTTL on PES substrate.

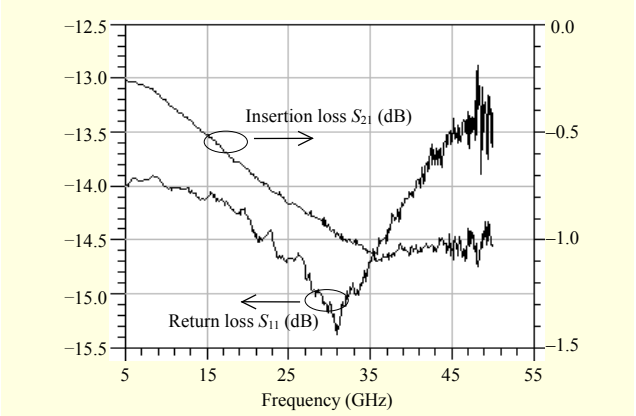

Fig. 16. Measured return loss S_{11} and insertion loss S_{21} of impedance transformer employing FTTL.

0.318 mm, which is 69.2% of the size of the transformer fabricated by the conventional coplanar waveguide on PES. In other words, if the $\lambda/4$ transformer with a Z_0 of 61 Ω is fabricated by the conventional coplanar waveguide on the PES substrate, then W is 0.27 mm, the length of the $\lambda/4$ signal line is 1.7 mm, and its size is 0.459 mm × 0.459 mm.

Figure 16 shows measured return loss S_{11} and insertion loss S_{21} of the transformer. The insertion and return loss are measured at a port impedance of 50 Ω, and it is normalized by the source impedance and load impedance, Z_{c1} and Z_{c2}. As shown in Fig. 16, there are excellent RF performances from the transformers. Concretely, we can observe return loss values better than –12.9 dB from 5 GHz to 50 GHz and insertion loss values better than –1.13 dB in the same frequency range. These results indicate that the FTTL is suitable for application to miniaturized flexible RF components on PES.

V. Conclusion

In this work, we fabricated a coplanar waveguide on a PES substrate for application to a flexible MMIC and thoroughly investigated its RF characteristics. According to the measured results, the coplanar waveguide on PES showed a very low loss compared with that which the conventional silicon substrate showed. Concretely, it showed an insertion loss lower than 0.7 dB/mm and an attenuation constant (α) lower than 0.085 Np/mm up to 50 GHz. The Q-factor of the coplanar waveguide on PES was 40.3 at a resonance frequency of 46.7 GHz. It showed a wavelength of 3.9 mm to 6.2 mm from 30 GHz to 50 GHz and an effective permittivity (ε_{eff}) of 2.35 to 2.97 from 10 GHz to 50 GHz. The coplanar waveguide on PES showed a very weak frequency dispersion characteristic compared with that of the silicon substrate. We also fabricated the FTTL structure on the PES substrate and investigated its RF characteristics. According to the results, the FTTL structure on PES showed much higher capacitance and inductance values than the conventional coplanar waveguide on PES showed due to additional C and L, which led to a high reduction of wavelength. Concretely, the wavelength of the FTTL on PES was 5.11 mm at 20 GHz, which was 55% of that of the conventional coplanar waveguide on PES. The characteristic impedance, Z_0, of the FTTL could be easily controlled by only changing the length of PMS, which indicates that miniaturized flexible RF components with various impedance values can be realized on the PES substrate by using the FTTL. The FTTL on PES also showed very low loss compared with that which the commercial silicon substrate showed due to the excellent electrical insulating properties of PES. In addition, the FTTL structure exhibited much higher propagation constant β and effective permittivity ε_{eff} than the conventional coplanar waveguide on PES exhibited due to its slow-wave mode characteristic originating from the periodic structure. Using the FTTL on PES, we fabricated an impedance transformer on the PES substrate for flexible MMIC applications. The impedance transformer was designed to transform an impedance of 75 Ω into a standard impedance of 50 Ω. The size of the impedance transformer was 0.318 mm × 0.318 mm, which was 69.2% of the size of the transformer fabricated by the conventional coplanar waveguide on the PES. We observed excellent RF performances from the impedance transformer. Concretely, we observed return loss values better than –12.9 dB from 5 GHz to 50 GHz and insertion loss values better than –1.13 dB in the same frequency range. These results indicate that PES is a promising candidate for application to flexible MMIC in the high frequency.

References

[1] Y. Yun et al., "A Study On RF Characteristics of Polyether Sulfone Substrate for Application to Flexible Mobile Communication Device," *Asia-Pacific Microw. Conf.*, Seoul, Rep. of Korea, Nov. 2013, pp. 881-883.

[2] M.S. Oh et al., "Low Voltage Complementary Thin-Film Transistor Inverters with Pentacene-ZnO Hybrid Channels on

AlO_X Dielectric," *Appl. Physics Lett.*, vol. 90, no. 17, Apr. 2007, pp. 173511:1-173511:3.

[3] Y.W. Choi et al., "Low-Voltage Organic Transistors and Depletion-Load Inverters with High-K Pyrochlore BZN Gate Dielectric on Polymer Substrate," *IEEE Trans. Electron Devices*, vol. 52, no. 12, Dec. 2005, pp. 2819-2824.

[4] Y. Sun and J.A. Rogers, "Inorganic Semiconductors for Flexible Electronics," *Adv. Mater.*, vol. 19, no. 15, Aug. 2007, pp. 1897-1916.

[5] Y.S. Chen, "IR Welding of Glass Filled Polyether Sulfone Composite," *Tamkang J. Sci. Eng.*, vol. 2, no. 4, 2000, pp. 229-234.

[6] E. Celik et al., "Carbon Nanotube Blended Polyethersulfone Membranes for Fouling Control in Water Treatment," *Water Research*, vol. 45, no. 1, Jan. 2011, pp. 274-282.

[7] H.L. Wu et al., "Preparation and Characterization of Poly(ether sulfone)/sulfonated Poly(ether ether ketone) Blend Membranes," *European Polymer J.*, vol. 42, no. 7, July 2006, pp. 1688-1695.

[8] R. Rajasekaran, M. Alagar, and C.K. Chozhan, "Effect of Polyethersulfone and *N, N'*-Bismaleimido-4, 4′-Diphenyl Methane on the Mechanical and Thermal Properties of Epoxy Systems," *eXPRESS Polymer Lett.*, vol. 2, no. 5, 2008, pp. 339-348.

[9] Y. Yun et al., "RF Characteristics of Coplanar Waveguide Fabricated on Flexible PES," *Microw. J.*, vol. 56, no. 2, Feb. 2013, pp. 90-100.

[10] H.-C. Yuan and Z. Ma, "Microwave Thin-Film Transistors Using Si Nanomembranes on Flexible Polymer Substrate," *Appl. Physics Lett.*, vol. 89, no. 21, Nov. 2006, pp. 212105:1-212105:3.

[11] Y. Yun, "Highly Miniaturized On-Chip 180° Hybrid Employing Periodic Ground Strip Structure for Application to Silicon RFIC," *ETRI J.*, vol. 33, no.1, Feb. 2011, pp. 13-17.

[12] J.R. Long, "Passive Components for Silicon RF and MMIC Design," *IEICE Trans. Electron.*, vol. E86-C, no. 6, June 2003, pp. 1022-1031.

[13] W.H. Haydl et al., "Millimeterwave Coplanar Transmission Lines on gallium arsenide, Indium Phosphide and Quartz with Finite Metallization Thickness," *IEEE MTT-S Int. Microw. Symp. Digest*, vol. 2, Boston, MA, USA, July 10-14, 1991, pp. 691-694.

[14] C.H. Doan et al., "Design of CMOS for 60 GHZ Applications," *Proc. IEEE Int. Solid-State Circuits Conf.*, Session 24.4, vol. 1, Feb. 15-19, 2004. pp. 440-538.

[15] T. Hirota, A. Minakawa, and M. Muraguchi, "Reduced-Size Branch-Line and Rat-Race Hybrids for Uniplanar MMIC's," *IEEE Trans. Microw. Theory Tech.* vol. 38, no. 3, Mar. 1991, pp. 270-275.

[16] J. Zhang and T.Y. Hsiang, "Dispersion Characteristics of Coplanar Waveguides at Subterahertz Frequencies," *Prog. Electromag. Research Symp.,* Cambridge, MA, USA, Mar. 26-29, 2006, pp. 232-235.

[17] D.M. Pozar, *Microwave Engineering*, Reading, MA: Addison-Wesley, 1990.

[18] B.C. Wadell, *Transmission Line Design Handbook*, Norwood, MA: Artech House, 1991.

Young Yun received his BS in electronics engineering from Yonsei University, Seoul, Rep. of Korea, in 1993, his MS in electrical and electronics engineering from Pohang University of Science and Technology, Pohang, Rep. of Korea, in 1995, and his PhD in electrical engineering from Osaka University, Osaka, Japan, in 1999. From 1999 to 2003, he worked as an engineer for the Matsushita Electric Industrial Company Ltd. (Panasonic), Osaka, Japan, where he was engaged in the research and development of monolithic microwave ICs (MMICs) for wireless communications. In 2003, he joined the Department of Radio Sciences and Engineering, Korea Maritime University, Busan, Rep. of Korea. He is currently a professor, and his research interests include design and measurement for RF/microwave and millimeter-wave IC and design and fabrication for HEMT and HBT. Since 2008, he has served as an associate editor of IEICE (The Institute of Electronics, Information and Communication Engineers) in Japan and an editor of the Korean Society of Marine Engineering in Korea. He is the author or co-author of over 110 internationally published journal articles and 15 patents pending in RF/microwave device and IC.

Hong Seung Kim received his BS, MS, and PhD in materials science and engineering from the Korea Advanced Institute of Science and Technology in 1990, 1993, and 1999, respectively. He joined ETRI, Daejeon, Rep. of Korea, in 1999 and has worked on the fabrication and development of SiGe heterojunction bipolar transistors (HBTs) and InP/InGaAs HBTs for OEIC. From 2001 to 2002, he was a postdoctoral research associate in electrical engineering at Cornell University, Ithaca, NY, USA, where he worked on three-dimensional integration. In 2003, he joined the Deptartment of Nano Semiconductor Engineering, Korea Maritime University, Busan, Rep. of Korea. He is currently a professor and his research interests include optoelectronic properties of ZnO-based devices, such as UV LEDs and transparent transistors.

Nakwon Jang received his BS, MS and PhD in electrical engineering from Yonsei University, Rep. of Korea, in 1990, 1992, and 1999, respectively. From 1992 to 1995, he was with Samsung Electronics, Rep. of Korea, where he was involved in the design of video signal driver circuits for p-Si TFT LCDs. After completing his PhD, he worked as a senior engineer in the semiconductor R&D division of Samsung Electronics, where was engaged in the research and development of 4-Mb and 32-Mb FRAM. He joined Korea Maritime University as a professor in the Deptartment of Electrical and Electronics Engineering in September 2003. He is currently a professor, and his research interests include the design and fabrication of LEDs and ZnO TFTs. He is the author or co-author of over 70 journal articles on semiconductor devices.